The Astrophysical Journal, 690:1068–1073, 2009 January 10 doi:10.1088/0004-637X/690/2/1068

HESS OBSERVATIONS OF THE PROMPT AND AFTERGLOW PHASES OF GRB 060602B

F. Aharonian[1,2], A. G. Akhperjanian[3], U. Barres De Almeida[4,28], A. R. Bazer-Bachi[5], B. Behera[6], M. Beilicke[7], W. Benbow[1], K. Bernlöhr[1,8], C. Boisson[9], V. Borrel[5], I. Braun[1], E. Brion[10], J. Brucker[11], R. Bühler[1], T. Bulik[12], I. Büsching[13], T. Boutelier[14], S. Carrigan[1], P. M. Chadwick[4], R. Chaves[1], L.-M. Chounet[15], A. C. Clapson[1], G. Coignet[16], R. Cornils[7], L. Costamante[1,29], M. Dalton[8], B. Degrange[15], H. J. Dickinson[4], A. Djannati-Ataï[17], W. Domainko[1], L. O'C. Drury[2], F. Dubois[16], G. Dubus[14], J. Dyks[12], K. Egberts[1], D. Emmanoulopoulos[6], P. Espigat[17], C. Farnier[18], F. Feinstein[18], A. Fiasson[18], A. Förster[1], G. Fontaine[15], M. Füssling[8], S. Gabici[2], Y. A. Gallant[18], B. Giebels[15], J. F. Glicenstein[10], B. Glück[11], P. Goret[10], C. Hadjichristidis[4], D. Hauser[1], M. Hauser[6], G. Heinzelmann[7], G. Henri[14], G. Hermann[1], J. A. Hinton[19], A. Hoffmann[20], W. Hofmann[1], M. Holleran[13], S. Hoppe[1], D. Horns[7], A. Jacholkowska[18], O. C. de Jager[13], I. Jung[11], K. Katarzyński[21], E. Kendziorra[20], M. Kerschhaggl[8], D. Khangulyan[1], B. Khélifi[15], D. Keogh[4], Nu. Komin[18], K. Kosack[1], G. Lamanna[16], I. J. Latham[4], J.-P. Lenain[9], T. Lohse[8], J. M. Martin[9], O. Martineau-Huynh[22], A. Marcowith[18], C. Masterson[2], D. Maurin[22], T. J. L. McComb[4], R. Moderski[12], E. Moulin[10], M. Naumann-Godo[15], M. de Naurois[22], D. Nedbal[23], D. Nekrassov[1], S. J. Nolan[4], S. Ohm[1], J.-P. Olive[5], E. de Oña Wilhelmi[17], K. J. Orford[4], J. L. Osborne[4], M. Ostrowski[24], M. Panter[1], G. Pedaletti[6], G. Pelletier[14], P.-O. Petrucci[14], S. Pita[17], G. Pühlhofer[6], M. Punch[17], A. Quirrenbach[6], B. C. Raubenheimer[13], M. Raue[1], S. M. Rayner[4], M. Renaud[1], F. Rieger[1], J. Ripken[7], L. Rob[23], S. Rosier-Lees[16], G. Rowell[25], B. Rudak[12], J. Ruppel[26], V. Sahakian[3], A. Santangelo[20], R. Schlickeiser[26], F. M. Schöck[11], R. Schröder[26], U. Schwanke[8], S. Schwarzburg[20], S. Schwemmer[6], A. Shalchi[26], H. Sol[9], D. Spangler[4], Ł. Stawarz[24], R. Steenkamp[27], C. Stegmann[11], G. Superina[15], P. H. Tam[6], J.-P. Tavernet[22], R. Terrier[17], C. van Eldik[1], G. Vasileiadis[18], C. Venter[13], J. P. Vialle[16], P. Vincent[22], M. Vivier[10], H. J. Völk[1], F. Volpe[15,29], S. J. Wagner[6], M. Ward[4], A. A. Zdziarski[12], and A. Zech[9]

[1] Max-Planck-Institut für Kernphysik, Heidelberg, Germany
[2] Dublin Institute for Advanced Studies, Ireland
[3] Yerevan Physics Institute, Armenia
[4] University of Durham, Department of Physics, UK
[5] Centre d'Étude Spatiale des Rayonnements, CNRS/UPS, Toulouse, France
[6] Landessternwarte, Universität Heidelberg, Königstuhl, Germany; phtam@lsw.uni-heidelberg.de
[7] Universität Hamburg, Institut für Experimentalphysik, Germany
[8] Institut für Physik, Humboldt-Universität zu Berlin, Germany
[9] LUTH, Observatoire de Paris, CNRS, Université Paris Diderot, France
[10] DAPNIA/DSM/CEA, CE Saclay, Gif-sur-Yvette, France
[11] Universität Erlangen-Nürnberg, Physikalisches Institut, Germany
[12] Nicolaus Copernicus Astronomical Center, Warsaw, Poland
[13] Unit for Space Physics, North-West University, Potchefstroom, South Africa
[14] Laboratoire d'Astrophysique de Grenoble, INSU/CNRS, Université Joseph Fourier, Grenoble, France
[15] Laboratoire Leprince-Ringuet, Ecole Polytechnique, CNRS/IN2P3, Palaiseau, France
[16] Laboratoire d'Annecy-le-Vieux de Physique des Particules, CNRS/IN2P3, Annecy-le-Vieux, France
[17] Astroparticule et Cosmologie, CNRS, Universite Paris 7, France, UMR 7164 (CNRS, Université Paris VII, CEA, Observatoire de Paris)
[18] Laboratoire de Physique Théorique et Astroparticules, CNRS/IN2P3, Université Montpellier II, Montpellier, France
[19] School of Physics & Astronomy, University of Leeds, UK
[20] Institut für Astronomie und Astrophysik, Universität Tübingen, Germany
[21] Toruń Centre for Astronomy, Nicolaus Copernicus University, Toruń, Poland
[22] LPNHE, Université Pierre et Marie Curie Paris 6, Université Denis Diderot Paris 7, CNRS/IN2P3, France
[23] Institute of Particle and Nuclear Physics, Charles University, Prague, Czech Republic
[24] Obserwatorium Astronomiczne, Uniwersytet Jagielloński, Kraków, Poland
[25] School of Chemistry & Physics, University of Adelaide, Australia
[26] Institut für Theoretische Physik, Lehrstuhl IV: Weltraum und Astrophysik, Ruhr-Universität Bochum, Germany
[27] University of Namibia, Windhoek, Namibia

Received 2008 February 25; accepted 2008 September 12; published 2008 December 2

ABSTRACT

We report on the first completely simultaneous observation of a gamma-ray burst (GRB) using an array of Imaging Atmospheric Cherenkov Telescopes, which is sensitive to photons in the very high energy (VHE) γ-ray range ($\gtrsim$ 100 GeV). On 2006 June 2, the *Swift* Burst Alert Telescope (BAT) registered an unusually soft γ-ray burst (GRB 060602B). The burst position was under observation using the High Energy Stereoscopic System (HESS) at the time the burst occurred. Data were taken before, during, and after the burst. A total of 5 hr of observations were obtained during the night of 2006 June 2–3, and five additional hours were obtained over the next three nights. No VHE γ-ray signal was found during the period covered by the HESS observations. The 99% confidence level flux upper limit (>1 TeV) for the prompt phase (9 s) of GRB 060602B is 2.9×10^{-9} erg cm^{-2} s^{-1}. Due to the very soft BAT spectrum of the burst compared with other *Swift* GRBs and its proximity to the Galactic center, the burst is likely associated with a Galactic X-ray burster, although the possibility of it being a cosmological GRB cannot be ruled out. We discuss the implications of our flux limits in the context of these two bursting scenarios.

Key words: gamma rays: bursts – gamma rays: observations
Online-only material: color figures

1. INTRODUCTION

Gamma-ray bursts (GRBs) are brief and intense flares of γ-rays. Without precedent in astronomy, they arrive from random directions in the sky and last typically $\sim$0.1−100 s (prompt emission; see Klebesadel et al. 1973; Fishman & Meegan 1995). The very nature of GRBs makes it operationally rather challenging to study their prompt phase simultaneously in any other wavelength.

The observed GRB properties are generally well explained by the *fireball* model, in which the emission is produced in relativistic shocks (Piran 1999; Zhang & Mészáros 2004; Mészáros 2006). In this standard model, the highly relativistic plasma, which emits the observed sub-MeV radiation, is expected to generate γ-rays up to the very high energy (VHE; $\gtrsim$ 100 GeV) regime, via inverse-Compton emission of electrons or proton-induced mechanisms (Zhang & Mészáros 2001; Pe'er & Waxman 2005; Asano & Inoue 2007; Fan et al. 2008). Therefore, the detection of gamma rays or sufficiently sensitive upper limits would shed light on our understanding of the current model. Some important yet largely unknown parameters in GRB models, such as the bulk Lorentz factor and the opacity of the outflow just after the acceleration phase, can be directly measured through high-energy (HE; $\gtrsim$ 100 MeV) and VHE γ-ray observations during the prompt phase of GRBs (Razzaque et al. 2004; Baring 2006).

There are two techniques used in VHE γ-ray astronomy to observe the prompt phase. The first technique is to slew quickly to the GRB position provided by a burst alert from satellites. This technique is used for Imaging Atmospheric Cherenkov Telescopes (IACTs), such as the High Energy Stereoscopic System (HESS), which have a field of view (FoV) of a few degrees. The MAGIC telescope, operating in this mode, was able to slew to the position of GRB 050713A, 40 s after the GRB onset, while the prompt keV emission was still active. A total of 37 minutes of observations were made and no evidence of emission above 175 GeV was obtained (Albert et al. 2006a). The rapid follow-up observations using this telescope of eight other GRBs show no evidence of VHE γ-ray emission from these GRBs during the prompt or the early afterglow phase (Albert et al. 2007). However, there is always a delay in time for IACTs operating in this GRB-follow-up mode, as long as the GRB position lies outside the camera FoV at the onset of the GRB. This results in an incomplete coverage of the GRB prompt phase.

The second technique is to observe a large part of the sky continuously, at the expense of much lower sensitivity than the IACT detectors. This technique is used, e.g., for the water Cherenkov detector Milagro, which works at higher energies than current IACTs. Since the effect of extragalactic background light (EBL) absorption increases with the energy of a γ-ray photon, the higher energy threshold of Milagro thus lowers its chance to detect VHE γ-rays from distant GRBs, when compared to IACT detectors. No evidence of VHE γ-ray emission was seen from 39 GRBs using this detector (Atkins et al. 2005; Abdo et al. 2007). Atkins et al. (2000) reported a possible VHE γ-ray enhancement coincident with GRB 970417A (with a post-trials probability 1.5×10^{-3} of being a background fluctuation) using Milagrito, the forerunner of Milagro.

[28] Supported by CAPES Foundation, Ministry of Education of Brazil.
[29] European Associated Laboratory for Gamma-Ray Astronomy, jointly supported by CNRS, and MPG.

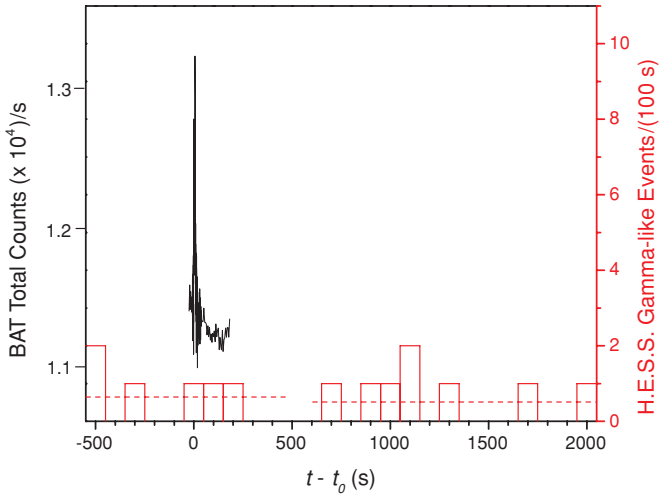

Figure 1. Histograms and right scale: Gamma-like events, i.e., those that passed standard cuts, as observed using HESS within a circular region of radius $\theta_{\rm cut} = 0.^{\circ}32$ (for $t < t_0 + 500$ s, with a large offset, see text) and $\theta_{\rm cut} = 0.^{\circ}11$ (for $t > t_0 + 600$ s) centered at the burst position. The dashed horizontal lines indicate the expected number of background events in the circular regions, using the reflected-region background model (Berge et al. 2007). The gap between $\sim$500 s and 600 s is due to a transition between observation runs. Solid curve and left scale: *Swift*/BAT light curve in the 15–150 keV band.

(A color version of this figure is available in the online journal.)

In this paper, we report on the first completely simultaneous observation with an IACT instrument of a γ-ray burst (GRB 060602B) using HESS. The burst position fell serendipitously at the edge of the FoV of the HESS cameras when the burst occurred.

2. GRB 060602B

At 23:54:33.9 UT on 2006 June 2 (denoted by t_0), the Burst Alert Telescope (BAT) on board *Swift*, which operates in the 15–350 keV energy band, triggered on GRB 060602B (trigger 213190; Schady et al. 2006). The refined BAT position was R.A. = $17^{\rm h}49^{\rm m}28.^{\rm s}2$, decl. = $-28^{\circ}7'15.''5$ (J2000; Palmer et al. 2006). The BAT light curve showed a single-peaked structure lasting from $t_0 - 1$ s to $t_0 + 9$ s (Figure 1). The peak was strongest in the 15–25 keV energy band and was not detected above 50 keV. T_{90} (defined as the time interval between the instants at which 5% and 95% of the total integral emission is detected in the 15–350 keV band) was 9 ± 2 s (Palmer et al. 2006). This $\sim$ 9 s time interval is referred to as the prompt phase of this GRB in this work. Palmer et al. (2006) fit the time-averaged energy spectrum from $t_0 - 1.1$ s to $t_0 + 8.8$ s by a simple power law with a photon index of 5.0 ± 0.52, placing it among the softest of the *Swift* GRBs. Using the data from the same time interval, a 15–150 keV fluence of $(1.8 \pm 0.2) \times 10^{-7}$ erg cm^{-2} was derived. No spectral evolution was observed during the burst (Wijnands et al. 2009).

Swift's other instrument, the X-ray Telescope (XRT), began data-taking 83 s after the BAT trigger and found a fading source. Beardmore et al. (2006) reported a position R.A. = $17^{\rm h}49^{\rm m}31.^{\rm s}6$, decl. = $-28^{\circ}8'3.''2$ (J2000), confirmed by later analyses (Butler 2007; Wijnands et al. 2009). This position (with an error circle of radius $\sim 3.''7$) was used in analyses presented in this paper. The flux faded temporally as a power law with an index of 0.99 ± 0.05 from $\sim t_0 + 100$ s up to $\sim t_0 + 10^6$ s (Wijnands et al. 2009).

Using data taken from $t_0 + 100$ s to $t_0 + 11.4$ ks, the time-averaged 0.3–10 keV energy spectrum was fitted by an absorbed

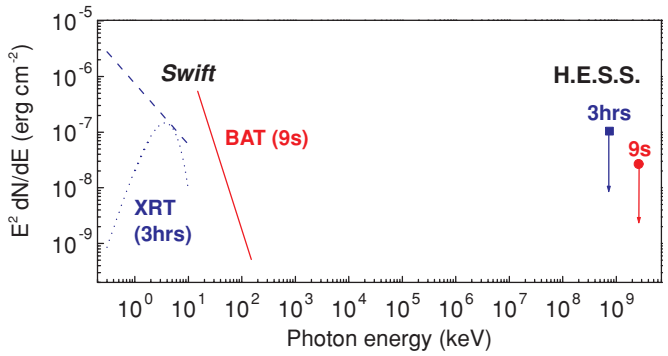

Figure 2. Time-integrated spectral energy distributions at the burst position during the 9 s prompt phase and during the 3 hr afterglow phase. A power-law model fitted to the BAT spectrum during the 9 s burst (solid line) is shown, as well as the source spectra used in an absorbed power-law model (dashed line) and an absorbed blackbody model (dotted line) to describe the XRT spectrum during 100 s–11.4 ks after the burst onset. The HESS upper limits derived from 9 s prompt data (circle) and 3 hr afterglow data (square) are also indicated. The HESS prompt and afterglow limits are plotted at the corresponding average photon energies.

(A color version of this figure is available in the online journal.)

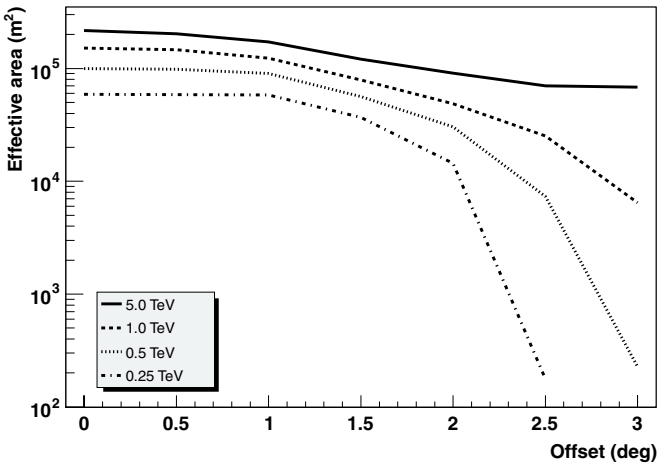

Figure 3. Effective areas for various photon energies at offsets from 0° to 3° from the center of the FoV for ZA = 0°, using the standard cut analysis used in this work.

power-law model, $dN/dE \propto E^{-\Gamma_X}$, where E is the photon energy in keV and Γ_X the photon index. The fit results in $\Gamma_X = 3.1^{+0.7}_{-0.6}$ and an absorption column density of $N_H = 4.6^{+1.6}_{-1.4} \times 10^{22}\mathrm{cm}^{-2}$, with $\chi^2/\mathrm{dof} = 34/35$. Fitting the same spectrum with an absorbed blackbody model, $dN/dE \propto E^2/[(kT)^4 (e^{E/kT} - 1)]$, a temperature of $kT = 0.94^{+0.15}_{-0.13}$ keV and $N_H = 1.5^{+1.0}_{-0.9} \times 10^{22}$ cm^{-2} were obtained, with $\chi^2/\mathrm{dof} = 36/35$. These two modeled source spectra are shown in Figure 2, for comparison with the HESS upper limits obtained over a comparable time interval. While the modeled *source* spectra look very different after different levels of absorption along the line of sight, they both describe the observed data equally well, as shown by the normalized χ^2 values both close to 1. These results are consistent with the analyses of other authors (Beardmore et al. 2006; Wijnands et al. 2009).

In the optical or IR band, no counterpart was found by the observations of several telescopes (Kubánek et al. 2006; Khamitov et al. 2006; Blustin et al. 2006; Melandri et al. 2006). This is expected because of the severe optical extinction along this line of sight.

3. THE HESS OBSERVATIONS

The HESS array is a system of four 13 m diameter IACTs located in the Khomas Highland of Namibia (Hinton 2004). The system has a point-source sensitivity above 100 GeV of $\sim 4 \times 10^{-12}$ erg cm^{-2} s^{-1} (about 1% of the flux from the Crab nebula) for a 5σ detection in a 25 hr observation. The cameras of the HESS telescopes detect Cherenkov photons over a 5° FoV, thus enhancing its ability to detect serendipitous sources, as demonstrated in the Galactic plane survey (Aharonian et al. 2005a).

The position of GRB 060602B was under observation using HESS before the burst, throughout the duration of the burst, and after the burst. The observations are shown in Table 1. The zenith angles (ZA) and the offsets of the GRB 060602B position from the center of the FoV are shown for each observation period. A total of 4.9 hr of observations were obtained during the night of 2006 June 2–3. This includes 1.7 hr *preburst*, 9 s prompt, and 3.2 hr *afterglow* phases. Additionally, 4.7 hr of observations at the burst position were obtained over the next three nights. All data were taken in good weather conditions and with good hardware status. The observations were taken with the GRB 060602B position placed at different offsets relative to the center of the FoV of the telescopes, because most observations were not dedicated to the position of GRB 060602B. The position offsets were rather large ($\geqslant 2.^\circ 5$) during the period before the burst until ~9 minutes after the burst.

Due to the HESS long-term monitoring program of the Galactic center region, a deep exposure of the GRB 060602B position (over a period of several years) also exists (see Section 5).

4. HESS DATA ANALYSIS

Calibration of data, event reconstruction, and rejection of the cosmic-ray background (i.e., γ-ray event selection criteria) were performed as described in Aharonian et al. (2006a), which employ the techniques described by Hillas (1996). Targets are typically observed at a normal offset from the FoV center of $0.^\circ 5$ or $0.^\circ 7$ (wobble mode), to allow for a simultaneous background estimate from regions in the FoV that have identical properties as the source position. At normal offsets, the point spread function (PSF) and effective area for γ-rays are nearly identical to the values at the FoV center, according to air-shower simulations. However, the reconstructed event directions are less accurate at larger offsets. The PSF at the maximum offset of $2.^\circ 9$ is by a factor of ~ 2 more extended than that at normal offsets. Figure 3 shows the effective areas for various photon energies at offsets from 0° to 3° from the center of the FoV for ZA= 0°, using the standard cut analysis described below.

Gamma-like events were then taken from a circular region of radius θ_{cut} centered at the burst position. The background was estimated using the reflected-region background model as described in Berge et al. (2007).

Two sets of analysis cuts were applied to search for a VHE γ-ray signal. These include standard cuts (Aharonian et al. 2006a) and soft cuts (with lower energy thresholds, as described in Aharonian et al. 2006b).[30] Standard cuts are optimized for a source with a photon index of $\Gamma = 2.6$. Soft cuts are optimized for sources with steep spectra ($\Gamma = 5.0$), thus having a better sensitivity at lower energies. The latter is useful for a source at cosmological distances, since the EBL absorption would greatly

[30] *Soft cuts* were called *spectrum cuts* in Aharonian et al. (2006b).

Table 1
HESS Observations at the Burst Position

Date[a]	T_{start}[b]	ZA[c]	Offset[d]	E_{th}[e]	f_{UL}[f] ($> E_{th}$)	f_{UL}[f] (> 1 TeV)
2	22:03:37	23.3	2.5	540	4.2 (7%)	1.6
2	22:33:48	16.5	2.5	540	11 (19%)	4.0
2	23:04:10	9.9	2.9	1170	5.5 (31%)	7.1
2	23:34:10	3.7	2.9	1060	3.3 (16%)	3.6
3	00:04:38	4.8	2.1	240	20 (11%)	2.0
3	00:34:38	10.6	2.1	260	5.2 (3%)	0.61
3	01:04:50	16.2	1.3	240	8.8 (5%)	0.91
3	01:22:02	22.1	0.5	280	6.1 (4%)	0.81
3	02:03:02	31.6	0.5	320	7.4 (6%)	1.2
3	02:33:28	38.3	0.5	460	5.8 (8%)	1.7
3	03:03:52	45.1	0.5	600	5.5 (11%)	2.4
3	23:17:39	7.4	1.0	220	11 (5%)	0.97
3	23:47:36	4.8	1.0	220	4.6 (2%)	0.41
4	00:17:46	8.5	1.3	240	9 (5%)	0.93
4	00:47:46	14.9	1.3	240	12 (6%)	1.2
4	23:41:41	4.5	1.2	220	9.3 (4%)	0.83
5	00:12:13	8.9	0.6	220	7 (3%)	0.60
5	00:42:12	15.1	0.6	240	8.4 (4%)	2.3
5	01:12:27	22.9	1.1	290	13 (9%)	1.8
6	00:36:42	15.0	0.4	240	15 (8%)	1.5
6	01:06:48	21.5	0.4	260	9.1 (5%)	1.1

Notes.
[a] Date in 2006 June.
[b] Start time of the observation in UT. All but the seventh observation run, which has an exposure of 14 minutes, have an exposure time of 28 minutes.
[c] Mean zenith angle of the observation run in degrees.
[d] Offset of the burst position from the center of the FoV in degrees.
[e] Energy threshold for a standard cut analysis in GeV.
[f] 99% flux upper limit for a standard cut analysis in 10^{-12} photons cm^{-2} s^{-1}, assuming a photon spectral index of 2.6, where numerals in brackets indicate the fractional flux in crab unit above the same threshold.

soften the intrinsic spectrum of the VHE γ-ray radiation from the source. For observational periods with a position offset of 2.°9, a larger θ_{cut} value of 0.°32 was used to accommodate the larger PSF. Energy thresholds (E_{th}) obtained for a standard cut analysis in each period are shown in Table 1.

Figure 1 shows the rate of γ-like events (i.e., those that passed standard cuts) observed within a circular region of radius $\theta_{cut} = 0.°32$ (for $t < t_0 + 500$ s) and $\theta_{cut} = 0.°11$ (for $t > t_0 + 600$ s) centered at the source.

The independent *Model* analysis technique (de Naurois 2005) was used to analyze the same data. The results obtained from both analyses are consistent with each other. Hence, only the analysis results based on Hillas parameters are presented in this paper.

5. RESULTS

No evidence for excess γ-ray events was found at any time before, during, or after the event GRB 060602B. A *Crab-like* photon spectral index of 2.6 is assumed when deriving the flux limits presented in this section. The 99% confidence level flux upper limits obtained by the method of Feldman & Cousins (1998) for every observation run using standard cuts are included in Table 1. Figure 4 shows the 99% energy flux upper limits above 1 TeV during the prompt and afterglow phases up to four nights after the burst. The energy flux limit (> 1 TeV) for the prompt phase of GRB 060602B is 2.9×10^{-9} erg cm^{-2} s^{-1}. The limits for the period $\sim 10^2$–10^4 s after the burst are at levels comparable to the X-ray energy flux as observed by *Swift*/XRT during the same period. These limits are not very sensitive to the assumed photon spectral index (within a factor of 2 when changing the index to 2 or 4).

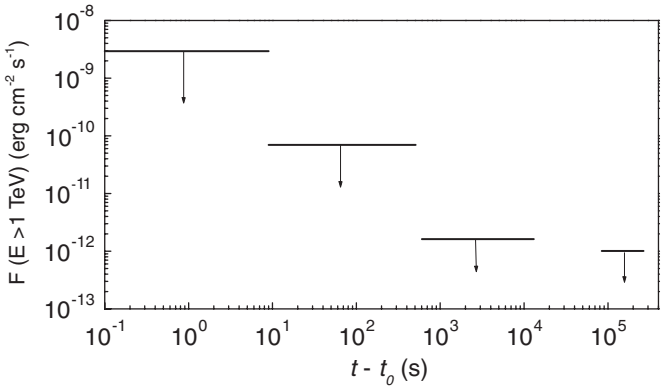

Figure 4. 99% confidence level flux upper limits at energies greater than 1 TeV derived from HESS observations at the position of GRB 060602B during the prompt and afterglow phases. The two ends of the horizontal lines indicate the start time and the end time of the observations from which the upper limits were derived.

HESS observations from 2004 to 2006 covering the position of GRB 060602B are used to constrain the time-averaged emission from this object. No signal was found in the 128 hr of available data, of which more than 80% were taken before the burst. Assuming constant emission, a 99% flux upper limit (using standard cuts) of 9.0×10^{-13} erg cm^{-2} s^{-1} above 200 GeV (about 0.5% of the Crab flux) was found. This result is relevant for the Galactic scenario discussed in Section 6.2.

Figure 2 shows the spectral energy distribution of the burst during the first 9 s, and during the period $t_0 + 100$ s to 11.4 ks ($\sim$ 3 hr) after the burst onset. It can be seen that the VHE energy fluence limits are of the similar level as the fluence at keV energies measured by *Swift* for both the 9 s prompt and 3 hr afterglow phases. Due to the soft keV spectra, any radiation in the VHE range would very likely come from a high-energy component separated from that of the sub-MeV radiation.

6. DISCUSSION

The nature of GRB 060602B is unclear. The softness of the BAT spectrum and the proximity of GRB 060602B to the Galactic center suggest a possible Galactic origin of the event. The observed temperature of $\sim$ 1 keV (using an absorbed blackbody fit) using XRT data is within the range seen from type-I X-ray bursts (Kuulkers et al. 2003). The *Swift*/BAT team has consequently classified the event as an X-ray burst (Barthelmy 2007). Halpern (2006) noted that a faint source had been visible in an *XMM-Newton* observation taken in the neighborhood of the GRB 060602B position. Two other *XMM-Newton* observations were performed almost 4 months after the burst and a faint source was detected. The position of the faint source is marginally consistent with the *Swift*/XRT position of GRB 060602B, within the large positional errors (up to 4″; Wijnands et al. 2009). However, no indication of variability of the source was seen and no secure spatial association of the source with GRB 060602B was established.

Although a Galactic origin is more likely, the possibility of the GRB as a cosmological GRB is not ruled out. In this section, we briefly discuss the implications of the HESS observations according to these two scenarios.

6.1. Implications for the Cosmological Gamma-ray Burst Scenario

HE γ-ray emissions have been detected in the prompt and/or afterglow phases of several GRBs (Hurley et al. 1994; González et al. 2003; Kaneko et al. 2008). In these cases, no evidence for a high-energy cut-off was seen. The temporal evolution of the HE emission of GRB 941017 was found to be significantly different from its low-energy γ-ray light curve (González et al. 2003). For GRB 970417A, if the excess events observed by Milagrito were actually associated with the burst, the photon energy must be at least 650 GeV and the VHE γ-ray energy fluence must be at least an order of magnitude higher than the 50–300 keV energy fluence as seen by BATSE (Atkins et al. 2003).

In the VHE regime, possible radiation mechanisms include leptonic scenarios—external-shock accelerated electrons upscattering self-emitted photons (Dermer et al. 2000; Zhang & Mészáros 2001) or photons from other shocked regions (Wang et al. 2001, 2006)—and hadronic scenarios—proton synchrotron emission (Böttcher & Dermer 1998; Totani 1998a, 1998b) or cascades initiated by π^0 produced via photo–meson interactions (Böttcher & Dermer 1998; Waxman & Bahcall 2000). In leptonic models, one typically expects a positive correlation between X-ray flux and VHE γ-ray flux. We note that the X-ray emission as seen by XRT decayed quickly, so one might expect the strongest VHE γ-ray emission to occur during the prompt phase or soon after. In fact, during the early afterglow phase, some authors predict VHE γ-ray energy flux levels comparable to or even higher than those in X-rays (Wang et al. 2001; Pe'er & Waxman 2005).

The energy threshold of the HESS observations was about 1 TeV and 250 GeV during the prompt and afterglow phases, respectively. For a cosmological GRB, VHE γ-ray radiation is attenuated by the EBL. The optical depth, τ, of the EBL absorption for a 1 TeV and 250 GeV photon is about unity at $z = 0.1$ and 0.3, respectively (Aharonian et al. 2006d). Therefore, if GRB 060602B occurred at $z \lesssim 0.2$, EBL absorption could be neglected. Under this assumption, the HESS flux limits would exclude an intrinsic VHE γ-ray prompt and afterglow energy fluence much higher than that at sub-MeV energies (see Figure 2). Also, a VHE γ-ray fluence level such as that implied by the possible γ-ray events associated with GRB 970417A would be excluded for GRB 060602B. And the upper limits would constrain models which predict VHE γ-ray energy flux levels higher than those in X-rays during $\sim 10^2$–10^4 s after the burst. If, however, GRB 060602B occurred at $z \gtrsim 0.2$, EBL absorption would be more severe and the observed limits would have to be increased by a factor which depends both on the redshift and the detailed gamma-ray spectrum of the GRB. In this case, the limits would be less constraining.

6.2. Implications for the Galactic X-ray Binary Scenario

X-ray binaries have been suspected to be VHE γ-ray emitters for decades (see e.g., the review by Weekes 1992) and have recently been confirmed for at least three cases (Aharonian et al. 2005b, 2006c; Albert et al. 2006b).

Type-I X-ray bursts, originating from low-mass X-ray binaries (LMXBs) and with typical duration of 10 s up to several minutes, are caused by thermonuclear flashes on the surface of accreting neutron stars[31] (Lewin et al. 1993). Although most X-ray bursts are detected from known X-ray sources or transients, some X-ray bursts originated from the so-called *burst-only* sources, whose quiescent X-ray luminosity is too low to be detected by current X-ray detectors (Cornelisse et al. 2004).

Based on the BAT spectrum of the burst and the possible identification of a faint *XMM-Newton* X-ray counterpart, Wijnands et al. (2009) prefer the type-I X-ray burst scenario. In this case, the source might have been active in X-rays before the BAT trigger, although there was no detection with the *Rossi X-Ray Timing Explorer*/All-Sky Monitor (*RXTE*/ASM) before the burst (Wijnands et al. 2009). The GRB 060602B position had been in the FoV of HESS for $\sim$2 hr when BAT triggered the event. No significant VHE γ-ray emission was observed during this period. If this scenario is true, the HESS observations rule out that this X-ray burst was accompanied by a VHE γ-ray burst of similar energy flux. To our knowledge, no simultaneous VHE γ-ray observation of a type-I X-ray burst has been reported. Aharonian et al. (1998) reported a tentative evidence of a possible TeV burst emission with HEGRA during radio/X-ray outbursts (on a scale of days) of the microquasar GRS 1915+105, which is a low-mass X-ray binary (LMXB) listed in Liu et al. (2001).

Persistent VHE γ-ray emission from LMXBs containing a neutron star was predicted (Király & Mészáros 1988; Cheng & Ruderman 1991). For example, particles can be accelerated in the vicinity of accreting neutron stars, giving rise to VHE γ-ray emission through interactions of ultra-high-energy nuclei with surrounding material. No steady VHE γ-ray emission of the progenitor of GRB 060602B was obtained from our long-term data. More than a dozen LMXBs (including GRS 1915+105) and

[31] This process was proposed to explain the origin of GRBs (see, e.g., Hameury et al. 1982; Woosley & Wallace 1982).

several high-mass X-ray binaries have also been observed with HESS and no detection was seen from any of them (Dickinson et al. 2008).

7. CONCLUSIONS

On 2006 June 2, the first completely simultaneous observations of a γ-ray burst (GRB 060602B) in hard X-rays and in VHE γ-rays with an IACT instrument were obtained.

The burst position was observed with HESS at VHE energies before, during, and after the burst. A search for a VHE γ-ray signal coincident with the burst event, as well as before and after the burst, yielded no positive result. The 99% confidence level flux upper limit (> 1 TeV) for the prompt phase of GRB 060602B is 2.9×10^{-9} erg cm^{-2} s^{-1}.

The nature of GRB 060602B is not yet clear, although a Galactic origin seems to be more likely. The complete and simultaneous coverage of the burst with an IACT instrument operating at VHE energies places constraints either in the Galactic X-ray binary scenario or the cosmological GRB scenario.

The support of the Namibian authorities and of the University of Namibia in facilitating the construction and operation of HESS is gratefully acknowledged, as is the support by the German Ministry for Education and Research (BMBF), the Max Planck Society, the French Ministry for Research, the CNRS-IN2P3 and the Astroparticle Interdisciplinary Programme of the CNRS, the UK Science and Technology Facilities Council (STFC), the IPNP of the Charles University, the Polish Ministry of Science and Higher Education, the South African Department of Science and Technology and National Research Foundation, and by the University of Namibia. We appreciate the excellent work of the technical support staff in Berlin, Durham, Hamburg, Heidelberg, Palaiseau, Paris, Saclay, and in Namibia in the construction and operation of the equipment. We acknowledge financial support by SFB 439. We thank an anonymous referee for a detailed report. This research has made use of data obtained from the High Energy Astrophysics Science Archive Research Center (HEASARC), provided by NASA's Goddard Space Flight Center. P. H. Tam thanks K. Arnaud and C. Gordan for assistance with the XRT analysis and acknowledges support from IMPRS-HD.

REFERENCES

Abdo, A. A., et al. 2007, ApJ, 666, 361
Aharonian, F. A., et al. 1998, Nucl. Phys. B, 60, 193 (HEGRA Collaboration)
Aharonian, F. A., et al. 2005a, Science, 307, 1938 (HESS Collaboration)
Aharonian, F. A., et al. 2005b, A&A, 442, 1 (HESS Collaboration)
Aharonian, F. A., et al. 2006a, A&A, 457, 899 (HESS Collaboration)
Aharonian, F. A., et al. 2006b, A&A, 448, L19 (HESS Collaboration)
Aharonian, F. A., et al. 2006c, A&A, 460, 743 (HESS Collaboration)
Aharonian, F. A., et al. 2006d, Nature, 440, 1018 (HESS Collaboration)
Albert, J., et al. 2006a, ApJ, 641, L9 (MAGIC Collaboration)
Albert, J., et al. 2006b, Science, 312, 1771 (MAGIC Collaboration)
Albert, J., et al. 2007, ApJ, 667, 358 (MAGIC Collaboration)
Asano, K., & Inoue, S. 2007, ApJ, 671, 645
Atkins, R., et al. 2000, ApJ, 533, L119
Atkins, R., et al. 2003, ApJ, 583, 824
Atkins, R., et al. 2005, ApJ, 630, 996
Baring, M. G. 2006, ApJ, 650, 1004
Barthelmy, S. D. 2007, GCN Circ., 6013 http://gcn.gsfc.nasa.gov/gcn3/6013.gcn3
Beardmore, A. P., Godet, O., & Sakamoto, T. 2006, GCN Circ., 5209, http://gcn.gsfc.nasa.gov/gcn3/5209.gcn3
Berge, D., Funk, S., & Hinton, J. A. 2007, A&A, 466, 1219
Blustin, A. J., Schady, P., & Pandey, S. B. 2006, GCN Circ., 5207, http://gcn.gsfc.nasa.gov/gcn3/5207.gcn3
Böttcher, M., & Dermer, C. D. 1998, ApJ, 499, L131
Butler, N. R. 2007, AJ, 133, 1027
Cheng, K. S., & Ruderman, M. 1991, ApJ, 373, 187
Cornelisse, R., et al. 2004, Nucl. Phys. B, 132, 518
de Naurois, M. 2005, in *Towards a Network of Atmospheric Cherenkov Detectors VII*, ed. B. Degrange & G. Fontaine (Palaiseau: École Polytechnique), 149
Dermer, C. D., Chiang, J., & Mitman, K. E. 2000, ApJ, 537, 785
Dickinson, H., et al. 2008, 30th ICRC Proc. submitted (arXiv:0710.4057, p.59)
Fan, Y.-Z., Piran, T., Narayan, R., & Wei, D.-M. 2008, MNRAS, 384, 1483
Feldman, G. J., & Cousins, R. D. 1998, Phys. Rev. D, 57, 3873
Fishman, G. J., & Meegan, C. A. 1995, ARA&A, 33, 415
González, M. M., Dingus, B. L., Kaneko, Y., Preece, R. D., Dermer, C. D., & Briggs, M. S. 2003, Nature, 424, 749
Halpern, J. 2006, GCN Circ., 5210, http://gcn.gsfc.nasa.gov/gcn3/5210.gcn3
Hameury, J. M., Bonazzola, S., Heyvaerts, J., & Ventura, J. 1982, A&A, 111, 242
Hillas, A. M. 1996, Space Sci. Rev., 75, 17
Hinton, J. A. 2004, NewA Rev., 48, 331
Hurley, K., et al. 1994, Nature, 372, 652
Kaneko, Y., Gonzalez, M. M., Preece, R., Dingus, B. L., & Briggs, M. S. 2008, ApJ, 677, 1168
Khamitov, I., Bikmaev, I., Sakhibullin, N., Aslan, Z., Kiziloglu, U., Gogus, E., Burenin, R., & Pavlinsky, M. 2006, GCN Circ., 5205, http://gcn.gsfc.nasa.gov/gcn3/5205.gcn3
Király, P., & Mészáros, P. 1988, ApJ, 333, 719
Klebesadel, R. W., Strong, I. B., & Olson, R. A. 1973, ApJ, 182, L85
Kubánek, P., Jelínek, M., & French, J. 2006, GCN Circ., 5199, http://gcn.gsfc.nasa.gov/gcn3/5199.gcn3
Kuulkers, E., den Hartog, P. R., in't Zand, J. J. M., Verbunt, F. W. M., Harris, W. E., & Cocchi, M. 2003, A&A, 399, 663
Lewin, W. H. G., van Paradijs, J., & van den Heuvel, E. P. J. 1993, Space Sci. Rev., 62, 223
Liu, Q. Z., van Paradijs, J., & van den Heuvel, E. P. J. 2001, A&A, 368, 1021
Melandri, A., et al. 2006, GCN Circ. 5229, http://gcn.gsfc.nasa.gov/gcn3/5229.gcn3
Mészáros, P. 2006, Rep. Prog. Phys., 69, 2259
Palmer, D., et al. 2006, GCN Circ. 5208, http://gcn.gsfc.nasa.gov/gcn3/5208.gcn3
Pe'er, A., & Waxman, E. 2005, ApJ, 633, 1018
Piran, T. 1999, Phys. Rep., 314, 575
Razzaque, S., Mészáros, P., & Zhang, B. 2004, ApJ, 613, 1072
Schady, P., Beardmore, A. P., Marshall, F. E., Palmer, D. M., Rol, E., & Sato, G. 2006, GCN Circ., 5200, http://gcn.gsfc.nasa.gov/gcn3/5200.gcn3
Totani, T. 1998a, ApJ, 502, L13
Totani, T. 1998b, ApJ, 509, L81
Wang, X. Y., Dai, Z. G., & Lu, T. 2001, ApJ, 556, 1010
Wang, X. Y., Li, Z., & Mészáros, P. 2006, ApJ, 641, L89
Waxman, E., & Bahcall, J. N. 2000, ApJ, 541, 707
Weekes, T. C. 1992, Space Sci. Rev., 59, 315
Wijnands, R., Rol, E., Cackett, E. M., Starling, R. L. C., & Remillard, R. A. 2009, MNRAS, in press (arXiv:0709.0061)
Woosley, S. E., & Wallace, R. K. 1982, ApJ, 258, 716
Zhang, B., & Mészáros, P. 2001, ApJ, 559, 110
Zhang, B., & Mészáros, P. 2004, Int. J. Mod. Phys. A., 19, 2385